

Bulk Properties of Pb-Pb collisions at $\sqrt{s_{NN}} = 2.76$ TeV measured by ALICE

Alberica Toia for the ALICE Collaboration

CERN Div. PH, 1211 Geneva 23

E-mail: alberica.toia@cern.ch

Abstract. Global variables, such as the charged particle multiplicity and the transverse energy are important observables to characterize Relativistic Heavy Ion collisions and to constrain model calculations. The charged particle multiplicity $dN_{ch}/d\eta$ and transverse energy $dE_T/d\eta$ are measured at $\sqrt{s_{NN}} = 2.76$ TeV in Pb-Pb collisions as a function of centrality and in pp collisions. The fraction of inelastic cross section seen by the ALICE detector is calculated either using a Glauber model or the data corrected by simulations of nuclear and electromagnetic processes, or data collected with a minimum bias interaction trigger. The centrality, defined by the number of nucleons participating in the collision, is obtained, via the Glauber model, by relating the multiplicity distributions of various detectors in the ALICE Central Barrel and their correlation with the spectator energy measured by the Zero-Degree Calorimeters. The results are compared to corresponding results obtained at the significantly lower energies of the BNL AGS, the CERN SPS, and the BNL RHIC, and with models based on different mechanisms for particle production in nuclear collisions. Particular emphasis will be given to a discussion on systematic studies of the dependence of the centrality determination on the details of the Glauber model, and the validity of the Glauber model at unprecedented collision energies.

1. Introduction: the importance of bulk properties

One fundamental element to study ultrarelativistic collisions is the characterization of the interaction in terms of bulk variables such as the transverse energy and the number of charged particles. These variables are closely related to the collision geometry and are important in understanding global properties of the system during the collision. This paper presents the first study of $dN_{ch}/d\eta$ at mid- and forward-rapidity and $dE_T/d\eta$ measured at $\sqrt{s_{NN}} = 2.76$ TeV by the ALICE experiment. The centrality dependence of these observables is characterized by the number of participants N_{part} , determined with a Glauber model of Pb-Pb collisions and is studied as a function of energy by comparing our results to those at RHIC and at the SPS. Finally, the results are compared to the available models. Charged particles N_{ch} and transverse energy E_T are generated by the initial scattering of the partonic constituents of the incoming nuclei and possibly also by reinteractions among the produced partons and hadrons. Without significant reinteraction, the observed transverse energy is the same as that produced by the initial

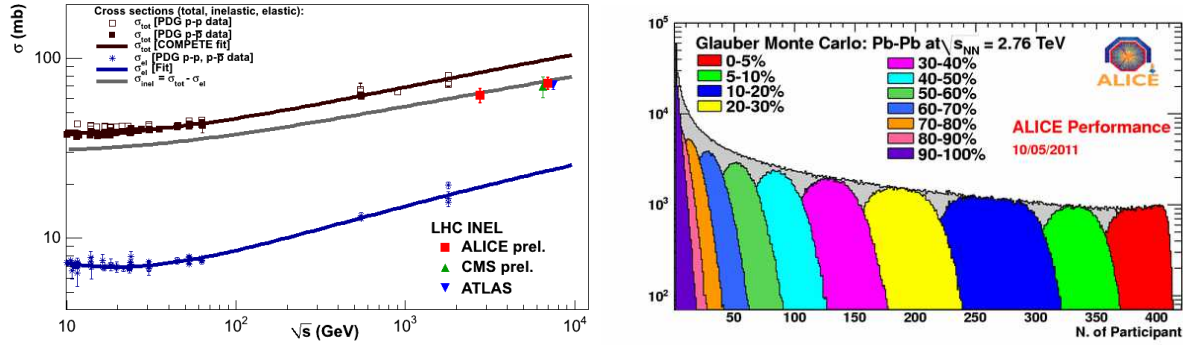


Figure 1: (left) World-data of total (squares) and elastic (star) cross sections in pp and $p\bar{p}$ collisions. The preliminary data from ALICE, ATLAS and CMS agree well with the extrapolation for the σ_{inel} . (right) Number of participants N_{part} for the centrality classes used in the analysis obtained for percentiles of the geometric cross section.

scattering. The amount of the reinteraction, and therefore of the equilibration of the fireball, can be measured evaluating the decrease of the initial scattering energy. To some extent transverse hydrodynamic flow can compensate this equilibrium. However gluon saturation can delay the onset of the flow reducing the effective pressure and thereby reducing the difference in the initially produced and the observed energy. The systematic study of global event properties, in particular transverse energy, charged multiplicity and mean transverse momentum, their centrality and energy dependence, may impose significant constraints on the collision dynamics.

2. Measurement of the centrality

ALICE has collected in the Pb-Pb run last year ~ 30 million events with nuclear collisions using minimum bias triggers with increasingly tighter conditions. These triggers use the VZERO scintillators (covering $2.8 < \eta < 5.1$ and $-3.7 < \eta < -1.7$) and Silicon Pixel Detector (SPD, $|\eta| < 1.4$)[1], and their efficiency ranges from 97 to 99%, as measured in simulations and dedicated pp runs taken with minimum interaction triggers. However peripheral collisions are strongly contaminated by electromagnetic (EM) background for which the cross sections are much higher than at the lower energies measured so far. QED processes and photo-nuclear interactions, where one photon from the EM field of one of the nuclei interacts with the other nucleus, possibly fluctuating to a vector meson yield soft particles at mid-rapidity [2]. At beam rapidity the cross section is large for electromagnetic dissociation, where one or both nuclei breaks up as a consequence of the EM interaction.

2.1. Glauber Model

Hadronic processes are described in a simple geometrical picture by the Glauber Model, which assumes straightline nucleon trajectories and N-N cross section independent of the number of collisions the nucleons have undergone before. The nuclear density profile

is given by a Woods-Saxon distribution. We used a nucleon-nucleon cross section, see Fig. 1 (left) of 64 mb, estimated from all available measurements (before LHC) [3] and now confirmed by measurements by ATLAS, CMS and ALICE ones, thanks to Van der Meer scans [4] and a detailed analysis of the diffractive systems [5]. The collision geometry determines the number of nucleons that participate in the reaction, so-called number of participants N_{part} , in Fig. 1 (right). The definition of centrality is based on the basic assumption that the impact parameter b is monotonically related to particle multiplicity or the energy produced at mid-rapidity.

2.2. Multiplicity distributions in the Central Barrel

The multiplicity distribution of any of these centrality observables has a classical shape. As an example, the distribution of VZERO amplitude is shown in Fig. 2 (left). The peak corresponds to most peripheral collisions (contaminated by EM background and by missing events due to the trigger efficiency), the plateau to the mid-central and the edge to the central collisions which results from the intrinsic fluctuations and the detector acceptance and resolution. Other observables include the number of Time Projection Chamber (TPC, $|\eta| < 0.9$) tracks and the number of SPD clusters. The VZERO distribution is fitted using a phenomenological approach based on the Glauber Monte Carlo plus a convolution of a model for the particle production and a negative binomial distribution (NBD). It is assumed that the number of independently decaying precursor particles (“ancestors”) is given by a 2 component model $N_{ancestors} = f \cdot N_{part} + (1 - f) \cdot N_{coll}$, where $f \sim 80$ % from the fit quantifies their relative contribution. Other ancestor dependences have been tested, using power-law functions of N_{part} or N_{coll} . The number of particles produced per precursor source was assumed to follow a NBD distribution. The fit is performed in a region corresponding to 88% of the total cross section to avoid the peak of contamination and inefficiency. Extracting the number of participants from the Glauber fit gives accesses directly to the N_{part} , nearly identical to the geometrical one. However it is important to remember that we use the Glauber model and the ancestor assumptions only to determine the fraction of total cross section that we see, confirming the results obtained with the data-based analysis.

2.3. Spectator measurement with the Zero Degree Calorimeter (ZDC)

Another way to determine the centrality is to measure the energy deposited by the spectators in the Zero Degree Calorimeter (ZDC). This in principle provides directly the number of participants, however the nuclear fragmentation breaks the simple relation in the measured variables. The ZDC therefore needs to be correlated to another detector, in this case the electromagnetic calorimeter ZEM. Since the ZDC is far from the interaction point and therefore rather independent on the vertex, this centrality measure is particularly suited for the analysis that does not require any vertex cut, and it gives good results for central collisions, where the ZDC signal is well correlated with

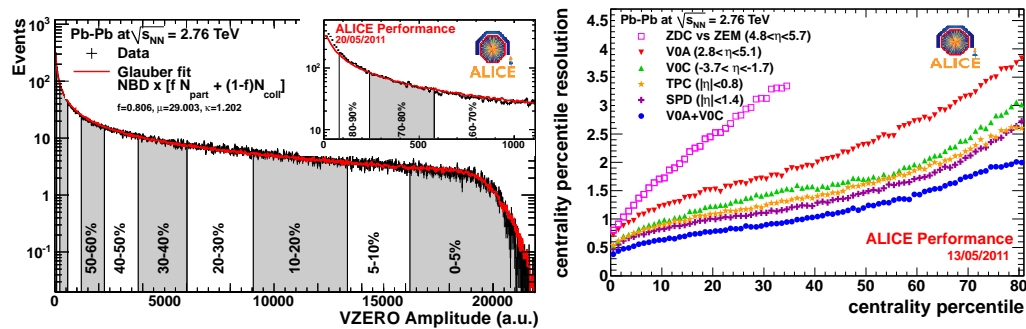


Figure 2: (left) Distribution of the sum of amplitudes in the VZERO scintillators. The line shows the fit of the Glauber calculation to the measurement. The centrality classes used in the analysis are indicated in the figure. The inset shows a zoom of the most peripheral region. (right) Centrality resolution for all the estimators evaluated in the analysis.

the number of spectators.

2.4. Centrality Resolution

We evaluated the performance of the centrality determination by comparing all our estimates. This is shown in Fig. 2 (right). The figure shows the RMS of the (Gaussian) distribution of $\sigma_i = cent_i - \langle cent \rangle$, where $\langle cent \rangle$ is calculated iteratively by

$$\langle cent \rangle = \frac{\sum cent_i / \sigma_i^2(cent_i)}{\sum 1 / \sigma_i^2(cent_i)} \quad (1)$$

The resolution depends on the rapidity coverage of the detector used. So when scaled by the square root of the N_{ch} measured in that detector all the results line up together. The resolution ranges from 0.5% in central to 2% in peripheral collisions.

3. Measurement of the charged particle multiplicity at mid-rapidity

The multiplicity of charged particles is measured at mid rapidity with an analysis based on SPD tracklets [6, 7]. Figure 3 (left) shows the charged particle pseudorapidity density per participant pair in $|\eta| < 1$ as a function of N_{part} . The Pb-Pb data points extrapolate well to the pp measurement. Compared to the RHIC results [8], also shown in the figure, there is an increase of about a factor 2.1, but the centrality trend looks very similar, at least for $N_{part} > 100$. Also the RHIC points match well the corresponding pp measurement [9]. One can observe a splitting in the centrality dependence for $N_{part} < 100$.

4. Estimate of the transverse energy

The transverse energy is estimated by measuring the charged hadronic energy with the tracking system corrected by the fraction of neutral particles not accessible by the tracking detectors. The total energy per participant pair is shown in Fig. 4 as a function

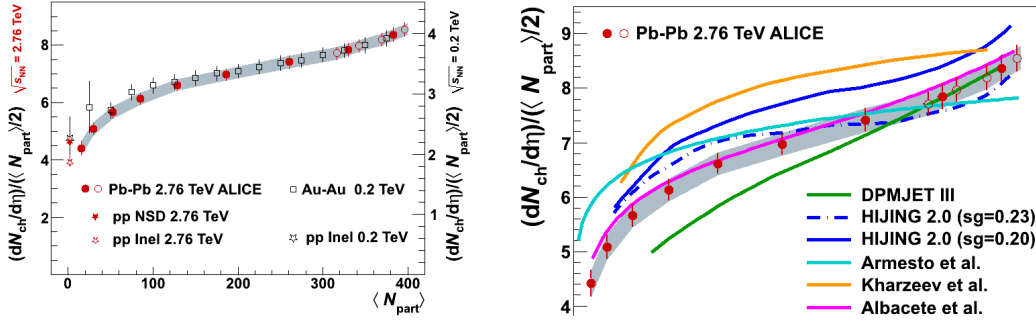


Figure 3: (left) Charged particle pseudo-rapidity density $(dN_{ch}/d\eta)/(\langle N_{part} \rangle/2)$ per participant pair as function of N_{part} for Pb-Pb collisions at 2.76 TeV and Au-Au collisions at 200 GeV (RHIC average) [8]. The scales for the different data sets are shown on the left and on the right respectively. The values for the pp collisions (LHC) are interpolations between data at 2.36 and 7 TeV. The pp value at RHIC energy is from [9]. (right) $(dN_{ch}/d\eta)/(\langle N_{part} \rangle/2)$ compared with model calculations (see Sec. 7).

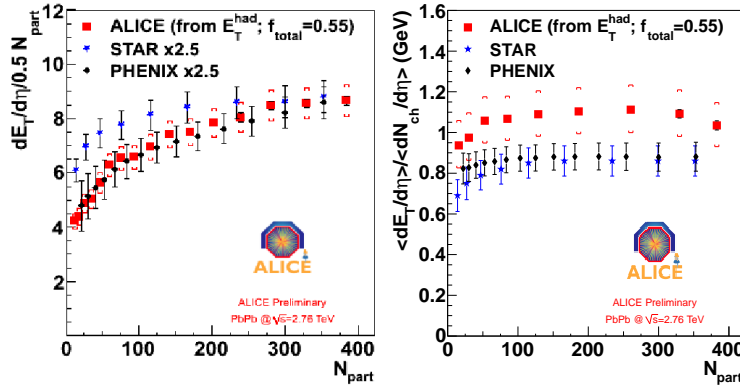


Figure 4: (left) Transverse energy per participant pairs $(dE_T/d\eta)/(\langle N_{part} \rangle/2)$ as function of N_{part} for Pb-Pb collisions at 2.76 TeV and Au-Au collisions at 200 GeV. The RHIC data are multiplied by a factor of 2.5 [8]. (right) Ratio of $(dE_T/d\eta)$ and $(dN_{ch}/d\eta)$ as function of N_{part} .

of N_{part} . As the multiplicity, it shows a steady rise with the number of participants, very similar to that shown at RHIC but increased by a factor of 2.5. This measurement can be used to extract the energy density using the Bjorken estimate

$$\epsilon = \frac{1}{\pi R^2 \tau} \frac{dE_T}{dy} \quad (2)$$

where τ is the formation time and πR^2 is the effective area of the collision. The most central (0-5%) value of dE_T/dy gives an $\epsilon\tau \sim 16$ GeV/(fm²c) at LHC, about a factor 3 larger than the corresponding one at RHIC [8]. Assuming that the multiplicity is proportional to the entropy of the final state, and that $\epsilon \propto T^4$, the factor 3 increase in energy density corresponds to a 30% increase in the temperature of the quark-gluon plasma produced in these collisions (at the same time after the onset of the reaction) compared with RHIC.

5. Energy dependence of $(dN_{ch}/d\eta)$ and $(dE_T/d\eta)$

The energy dependence is analyzed by comparing the results in the most central (0-5%) centrality bin at LHC energy with those for the same centrality bin at lower energy

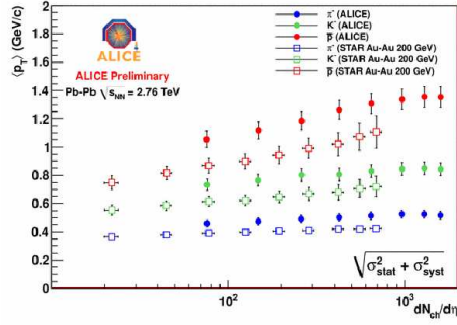


Figure 5: Mean p_T as a function of charged-particle density of identified hadrons (π, K, p) measured by ALICE at LHC energy of 2.76 TeV and by PHENIX and STAR at RHIC in Au-Au collisions at 200 GeV

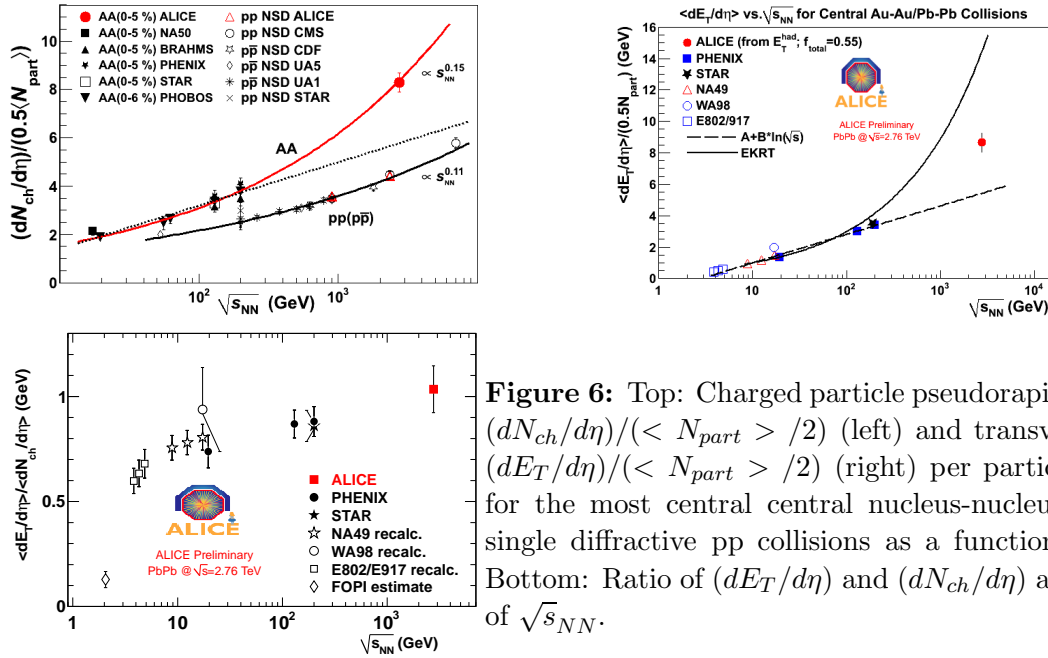


Figure 6: Top: Charged particle pseudorapidity density ($dN_{ch}/d\eta$)/($\langle N_{part} \rangle / 2$) (left) and transverse energy ($dE_T/d\eta$)/($\langle N_{part} \rangle / 2$) (right) per participant pairs for the most central central nucleus-nucleus and non-single diffractive pp collisions as a function of $\sqrt{s_{NN}}$. Bottom: Ratio of ($dE_T/d\eta$) and ($dN_{ch}/d\eta$) as a function of $\sqrt{s_{NN}}$.

[8]. Note that in contrast to RHIC data, our results are corrected for contamination by weak decay products. Fig. 6 (top left panel) shows that the charged particle multiplicity increases by a factor 2.1 with respect to RHIC data, but only by 1.9 in pp collisions at similar energy. The growth with energy is therefore different in pp and AA collisions, confirming the interplay of N_{part} and N_{coll} dependence in the particle production mechanism in heavy ion collisions. The increase in transverse energy (top right panel) is a factor 2.7 (consistent with the 2.5 reported on Fig. 4 and a 5% increase on the N_{part} with respect to RHIC), consistent with the observed increase of the mean particle momentum (see Fig. 5).

The energy dependency of both ($dE_T/d\eta$) and ($dN_{ch}/d\eta$) exhibits a power-law scaling (indicated by the red line in Fig. 6 top left panel) stronger than the logarithmic scaling (dotted lines in Fig. 6 top panels) suggested by the lower energy experiments. The centrality evolution looks similar for energy and multiplicity: both increase with energy and with centrality. Taking the ratio of ($dE_T/d\eta$) to ($dN_{ch}/d\eta$) (see Fig. 4 (right panel)) one can confirm the consistent behavior of the two observables as the ratio E_T/N_{ch} is rather independent on centrality, as was at RHIC, and slightly increases with

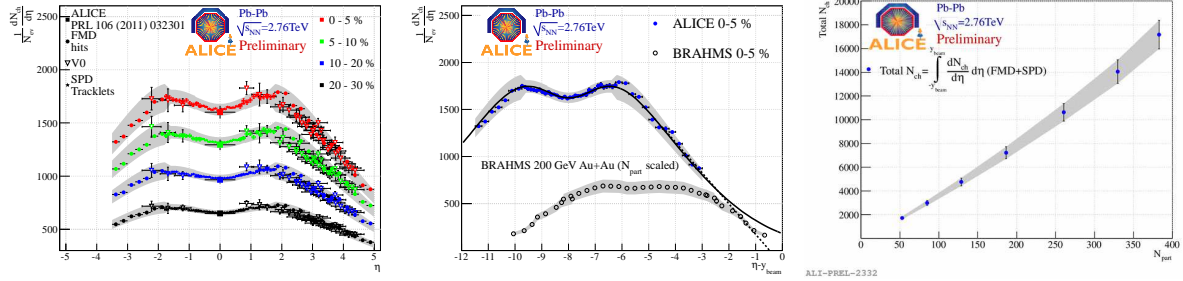


Figure 7: (left) $dN_{ch}/d\eta$ as a function of η measured by the SPD (at mid-rapidity) FMD and VZERO detector (at forward-rapidity). (middle) The most central $dN_{ch}/d\eta$ as a function of $\eta - y_{beam}$. The data are fitted to a Gaussian and a linear fit. Also included in the figure is BRAHMS data for Au-Au collisions at 200 GeV. (right) Total number of charged particles N_{ch} as a function of N_{part} .

energy (see Fig. 6 (bottom panel)).

6. Measurement of the charged particle multiplicity at forward-rapidity

Observables at forward rapidity are interesting probes of the properties of the initial state conditions, as for example the gluon density or the Color Glass Condensate. We measured the rapidity dependence of the charged particle multiplicity, by extending the rapidity coverage of the SPD measurement at mid-rapidity and complementing it with two analyses at forward rapidity with the VZERO and the FMD detector. The distributions are shown in Fig. 7 (left) for different centrality classes and the three measurements performed are in good agreement with each other. The particle multiplicity integrated in a given rapidity range increases with centrality with the same trend as the mid-rapidity data. Yields at high rapidity are expected to be independent of the energy, when viewed in the rest frame of one of the colliding nuclei. So we compared our measurements with the ones at RHIC from the BRAHMS experiment by shifting the rapidity by the beam rapidity (see Fig. 7 (middle)). We extend our measurement with two extrapolations, a double Gaussian and a linear extrapolation. From the comparison of the two energies it seems that the extended longitudinal scaling may work even at LHC energies. Thanks to those extrapolations we have calculated the total charged particle multiplicity, N_{tot} . N_{tot} is proportional to the number of participants N_{part} (see Fig. 7 (right)), indicating that the pseudorapidity distributions get narrower for more central collisions so that the width times the height of those distributions is approximately constant with centrality, i.e. that the increased particle production occurs mostly at mid-rapidity.

7. Interpretation, discussion and outlook

This paper presents a summary of the first results on global event properties measured by the ALICE Collaboration. ALICE has measured the charged particle pseudorapidity

density at mid- and forward rapidity and estimated the transverse energy. The yields per participant pairs show a consistent steady increase from peripheral to central both for $dN_{ch}/d\eta$ and $dE_T/d\eta$. The centrality dependence is strikingly similar to the one observed at RHIC energies. Taking into account the measurements at lower energy, the $\sqrt{s_{NN}}$ phenomenologically exhibits a power law scaling, stronger than the logarithmic scaling proposed earlier both for $dN_{ch}/d\eta$ and $dE_T/d\eta$. The ratio E_T/N_{ch} is flat with centrality, and its increase in energy with respect to the top RHIC energy is consistent with a 20% increase in the mean transverse momentum. The Bjorken energy density is increased by about a factor 3 from the top RHIC energy. In Fig. 3 the data have been compared to model calculations that describe RHIC measurements at $\sqrt{s_{NN}} = 200$ GeV and for which predictions at $\sqrt{s_{NN}} = 2.76$ TeV were available (see [6, 10] for a full comparison). The various models can be schematically divided in (i) the perturbative-QCD-inspired Monte Carlo, based on HIJING, tuned to 7 TeV pp data. This type of models typically have a soft component proportional to N_{part} and a hard component proportional to N_{coll} , partly motivating the parametrization used for the ancestors (see Fig. 2). Those models also include a strong impact parameter dependence of parton shadowing, the one for quarks fixed by the experimental data on DIS, the one from gluons determined by the centrality dependence in heavy-ion collisions. Others, (ii) so-called saturation model, also rely on pQCD and use an initial-state gluon density to predict some energy-dependent scale where quark and gluon density saturates therefore limiting the number of produced partons, and in turn, of particles. This results in a factorization of the energy and the centrality dependence of the multiplicity, observed in the experimental data. In general theoretical models need some sort of moderation mechanism to describe the centrality and energy evolution of the multiplicity. Further constraints can be imposed on models when describing also the forward rapidity region as well as the transverse energy together.

References

- [1] K. Aamodt et al. (ALICE), JINST 3, S08002 (2008).
- [2] O. Djuvsland, J. Nystrand, arXiv:1011.4908 (2010) and C. Oppedisano (ALICE Collaboration), these proceedings.
- [3] D. d’Enterria and K.Reygers, <https://twiki.cern.ch/twiki/bin/view/Main/LHCGlauberBaseline>, to be published.
- [4] K. Oyama (ALICE Collaboration), these proceedings.
- [5] M. Poghosyan (ALICE Collaboration), these proceedings.
- [6] K. Aamodt et al. (ALICE), Phys. Rev. Lett. 106, 032301 (2011).
- [7] C. Loizides (ALICE Collaboration), these proceedings.
- [8] S.S. Adler et al. (PHENIX), Phys. Rev. C71, 034908 (2005).
- [9] B.B. Back et al. (PHOBOS), Phys. Rev. C83, 024913 (2011).
- [10] K. Aamodt et al. (ALICE), Phys. Rev. Lett. 105, 252301 (2010).